International Journal of Heat and Mass Transfer 86 (2015) 820–825

Contents lists available at ScienceDirect

International Journal of Heat and Mass Transfer

journal homepage: www.elsevier.com/locate/ijhmt

Effects of radiation on the uncertainty of flame speed determination using spherically propagating flames with $CO/CO_2/H_2O$ dilutions at elevated pressures

Chae Hoon Sohn [a,*], Zheng Chen [b], Yiguang Ju [c]

[a] Department of Mechanical Engineering, Sejong University, Seoul 143-747, Republic of Korea
[b] SKLTCS, Department of Mechanics and Engineering Science, College of Engineering, Peking University, Beijing 100871, China
[c] Department of Mechanical and Aerospace Engineering, Princeton University, Princeton, NJ 08544, USA

ARTICLE INFO

Article history:
Received 14 August 2014
Received in revised form 12 March 2015
Accepted 17 March 2015

Keywords:
Radiation
Spherically propagating flame
Negative burned gas velocity
Density ratio
Elevated pressure

ABSTRACT

This work investigates numerically the effects of spectral dependent radiation on laminar flame speed determination using spherically propagating CH_4/air and H_2/air flames with $CO/CO_2/H_2O$ dilutions at elevated pressures. Three different models, adiabatic, optically thin radiation, and fitted statistically narrow band correlated k (FSNB-CK) models, are employed. The effects of radiation-induced negative burned gas velocity, increased density ratio, and chamber confinement induced flow compression are investigated. It is found that compared to the FSNB-CK model, the adiabatic flame model over-predicts the flame speed by 7% and the optically thin model makes more significant under-prediction. Moreover, this discrepancy increases with pressure. The results also show that a large negative velocity in the burned gas is induced by radiative heat loss and magnified further by the flow compression in a small combustion chamber. The radiation-induced negative burned gas velocity causes an under-estimation of flame speed. Moreover, radiation also increases the density ratio between the burned and the unburned gases. The use of the density ratio of adiabatic flame also causes under-prediction of flame speed. Two radiation corrections taking into account of the negative burned gas velocity and the increased density ratio are recommended for flame speed determination using propagating spherical flame for radiative mixtures. The corrections proposed in this study reduce the uncertainty of flame speed due to radiation.

1. Introduction

To achieve higher efficiency and lower emissions, future engines have to run at higher pressures with more exhaust gas recirculation or highly H_2O/CO_2 diluted syngas mixtures [1–3]. Development of validated high-pressure kinetic mechanisms with excessive H_2O/CO_2 dilution is important for quantitative prediction of ignition, heat release rate, flashback, and emissions in engines. Recently, significant progress has been made to develop high-pressure chemical kinetics for syngas and small hydrocarbons [4,5]. However, as shown in [6–8], the uncertainty of the existing kinetic mechanisms at high pressure is still very large and accurate measurement of laminar flame speeds at high pressure (above 10 atm) is critical to the development and validation of kinetic mechanisms.

Due to the strong hydrodynamic flame instability, most high-pressure flame speeds are measured using spherically propagating flames [9]. This method requires several assumptions to extrapolate stretched flame speed to unstretched one: zero burned gas velocity [10], linear/nonlinear relationship between stretched flame speed and stretch rate [11,12], adiabaticity of the flame, and constant density ratio of burned to unburned gas (ρ_b/ρ_u). The first assumption breaks up due to flow compression when the flame radius is larger than 30% of the chamber radius [10]. The second assumption becomes questionable when the mixture Lewis number deviates significantly from unity. The third and fourth assumptions may not be valid when radiation heat loss or absorption becomes significant. For example, the radiation cooling of burned gas causes flow contraction, which makes experimentally measured flame speed without radiation correction lower than the true value. Moreover, at excessive EGR conditions, radiation reabsorption of H_2O/CO_2 reduces the radiation heat loss or even increases the enthalpy of unburned gas and the flame speed [13–15]. However, few studies have been carried out to examine

* Corresponding author.
E-mail address: chsohn@sejong.ac.kr (C.H. Sohn).

http://dx.doi.org/10.1016/j.ijheatmasstransfer.2015.03.062
0017-9310/

the radiation effects on the determination of high-pressure flame speeds using a spherical bomb.

The effects of radiation on laminar flame speed measurement were first studied for spherical methane/air flames near the lean flammability limit [16]. It was found that radiation reduces the flame temperature and induces inward flow of burned gas, both of which slow down the flame propagation. Radiation was shown to cause up to 25% under-prediction of laminar flame speed. However, only atmospheric pressure condition was considered in this study and the results at high pressure were not explored. More recently, a semi-analytical investigation of radiation heat loss on the uncertainty of measured high pressure flame speeds was conducted [17]. The study concluded that the high pressure flame speeds of $H_2/He/O_2$ are only slightly affected by radiation, and that flames with low flame speeds are strongly affected by radiative loss. However, in the study, only optically thin radiation without any EGR effect was considered. It is well-known that radiation absorption affects not only the temperature distribution in the burned gas but also the flame propagation speed [13]. Currently, it is not clear how radiation absorption affects the flame speed determination in a high pressure spherical bomb when EGR compositions such as H_2O/CO_2 are present in the unburned mixtures. Moreover, it is not known how the negative flow velocity in the burned gas affects the flame speeds and whether the constant density ratio assumption is still valid in the presence of radiation.

The goal of this study is to provide quantitative assessment on which uncertainties need to be considered and how large they are for the determination of flame speeds of CH_4 and H_2 mixtures with $CO/CO_2/H_2O$ dilutions at pressures from 1 to 50 atm. The effects of radiation on flame propagation are modeled by including spectral dependent radiation emission and absorption as well as detailed chemistry and transport. Two radiation corrections taking into account of negative burned gas velocity and increased density ratio are proposed to achieve accurate flame speed determination from spherically propagating flames.

2. Numerical methods

The governing equations of one-dimensional, unsteady, compressible, multi-species reactive flow in a spherical coordinate are solved by using the Adaptive Simulation of Unsteady Reactive Flow solver (A-SURF 1D) code [18]. The details on governing equations, numerical schemes, code validations can be found in [18–20].

For radiation modeling, two different models, the optically thin model [21,22] and the fitted statistically narrow band correlated k (FSNB-CK) model [14,23], were employed to examine the effect of radiation heat loss and radiation absorption on flame speed measurements, respectively. For the optically thin model, the volumetric radiation heat loss was evaluated by

$$q_r = -4\sigma K_p(T^4 - T_\infty^4), \tag{1}$$

where σ is the Stefan–Boltzmann constant, K_p denotes Planck mean absorption coefficients of the mixture, and T and T_∞ are the local and the ambient temperatures, respectively. Four major radiative species of CH_4, CO_2, CO, and H_2O are considered and K_p was determined by using the high temperature SNB database [21]. For the FSNB-CK model [14,23], the radiation transfer was solved in the spherical coordinate using the S6 discrete ordinate method [13,14,24–26]. The average radiation intensity at each narrow band was calculated from the fitted cumulative k distribution function [14].

In this study, we considered two different radiative CO_2 and H_2O diluted mixtures, $0.083CH_4 + 0.275O_2 + 0.183He + 0.459CO_2$ (its equivalence ratio is $\varphi = 0.6$) [14] and $0.0594H_2 + 0.0594CO + 0.0699O_2 + 0.6613He + 0.1500H_2O$ ($\varphi = 0.85$) [8], which were experimentally studied using spherically propagating flames. GRI-MECH 3.0 [27] and Li et al.'s mechanisms [28] were used for methane and syngas flames, respectively. The detailed thermodynamic and transport properties are evaluated from the CHEMKIN packages [29]. The initial pressure was varied from 1 to 50 atm for methane flame and from 1 to 6 atm for syngas flame. To resolve the moving flame front, a dynamically adaptive mesh refinement algorithm with the minimum grid size of 7.8 μm was employed.

To examine the effect of flow compression [10,16] and its coupling with radiation on flame speed measurements, two different spherical chamber radii of 10 and 50 cm were used. The mixture was quiescent initially. To initiate flame kernel, a hot spot with radius of 1.5 mm and temperature of 1800 K, was used in the center of the chamber. The trajectory of flame front, R_f, defined as the position of maximum heat release rate, is monitored during flame propagation. When the zero burned gas velocity is assumed, the stretched flame speed, S_b, is equal to the flame propagation speed, i.e., $S_b = dR_f/dt$. The unstretched flame speed is obtained by linearly extrapolating S_b to zero stretch rate, $K = (2/R_f)(dR_f/dt)$.

3. Results and discussion

3.1. Flame Propagation Speeds in an Optically Thick $CH_4/O_2/He/CO_2$ Mixture

The optical thickness of the $CH_4/O_2/He/CO_2$ mixture is around 2.0 at 1 atm. The spherical flame propagation of the mixture is calculated for pressures from 1 to 50 atm in a chamber with radius between 10 and 50 cm. Its initial temperature is 298 K and the Lewis number for CH_4 in the mixture is about 1.2.

Fig. 1 shows the flame front trajectories at different pressures predicted by three different radiation models. It is observed that radiation model has a significant impact on the predicted flame trajectory. At all pressures, the adiabatic model predicts the fastest flame trajectory and the optically thin model predicts the slowest one. The trajectory predicted by the FSNB-CK model is between them, but it is more close to that of the adiabatic model. The dependence of the stretched burned gas flame speeds, S_b, on flame stretch, K, at 1 atm is also inserted in Fig. 1. The stretched burned gas flame speed is shown to have a good linear dependence on

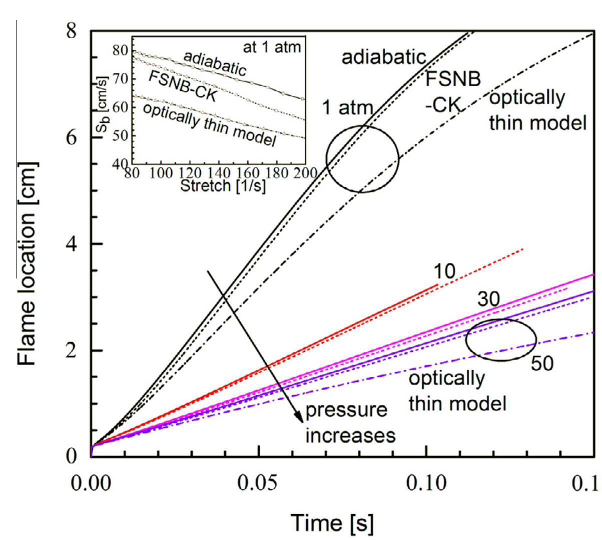

Fig. 1. Flame locations as a function of time from 1 to 50 atm during propagation of $CH_4/O_2/He/CO_2$ flames in a spherical chamber of 10 cm radius.

stretch rate, which allows us to extract the unstretched flame speed, S_b^o, according to the following linear correlation

$$S_b = S_b^o - L_b K, \tag{2}$$

where L_b denotes the Markstein length of burned gas.

The extrapolated unstretched flame speeds at different pressures are shown in Fig. 2, where the flame speed decreases monotonically with pressure. Moreover, the flame speeds predicted by the FSNB-CK model are very close to those of the adiabatic flames at all pressures, indicating that pressure changes slightly radiation effect on flame speed determination. However, the optically thin model significantly under-predicts the flame speeds and the magnitude of the under-prediction increases with pressure. The results suggest that for an optically thick mixture, the optically thin radiation model is not applicable to the prediction of flame speed measurement without appropriate corrections. On the other hand, the assumption of adiabatic flame without consideration of flame radiation is more appropriate to extrapolate the flame speed. However, care may be needed when mixtures with different flame speeds and optical thickness are considered.

Radiation absorption is a strong function of optical thickness. To examine the effect of optical thickness, calculations are made for chamber radius of 50 cm (five times increase in optical thickness). The comparison between flame trajectories for two different chamber radii, R_{ch} = 10 and 50 cm, and the dependence of S_b on stretch are shown in Fig. 3. The flame location is normalized by each chamber radius for generalization. The chamber size has an impact on flame trajectory. For R_{ch} = 10 cm, the predicted flame trajectories deviate from the linear trajectory at a much shorter time (0.08 s) than that with 50 cm in radius. The deviation becomes more significant as the flame radius increases, especially for the optically thin model. The inserted figure shows that chamber size changes the predicted flame speeds even at high stretch rates. For stretch rate below 70 s^{-1}, S_b shows a nonlinear dependence on stretch rate for R_{ch} = 10 cm. However, the nonlinear dependence for R_{ch} = 50 cm appears at much smaller stretch around 20 s^{-1}, allowing better extrapolation to get S_b^o

The nonlinear dependence of S_b is caused by two different effects, flow compression [10] and radiation cooling [16,17] effects. The flow compression induces an inward burned-gas flow in the opposite direction to flame propagation, i.e., a negative burned gas velocity behind the flame front. With the decrease of chamber

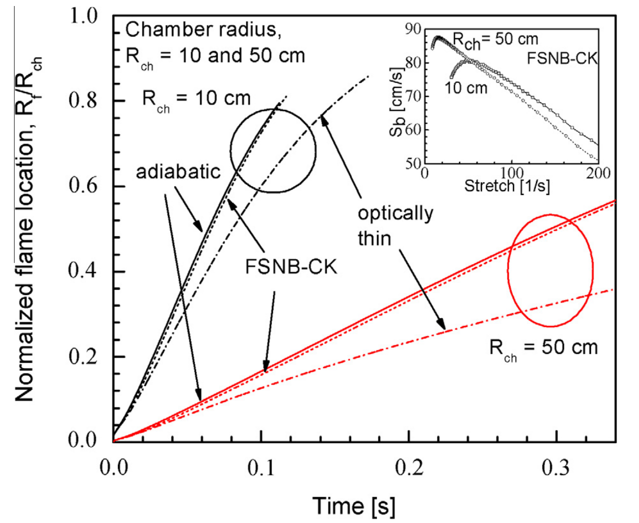

Fig. 3. Flame locations as a function of time at 1 atm calculated with three models of radiative heat loss, adiabatic, FSNB-CK, and optically thin models for $CH_4/O_2/He/CO_2$ flames in spherical chambers with radii of 10 and 50 cm.

size, the compression effect becomes stronger and the negative burned gas velocity increases [10]. As such, a smaller chamber has a larger negative burned gas velocity, which results in earlier nonlinear dependence of S_b on stretch at larger stretch rate (Fig. 3). For an adiabatic flame, this effect can be corrected using the Compression-Corrected Flame Speed (CCFS) [10].

However, for radiative flames, flow compression and radiation cooling are coupled and make the correction more complicated because radiation affects not only the negative burned gas velocity but also the burned gas temperature, leading to an increase in density ratio between burned and unburned gases. The determination of the laminar flame speed relative to unburned mixture, S_L^o, from S_b is linearly scaled by the density ratio,

$$S_L^o = \frac{\rho_b}{\rho_u}(S_b - u_b)^o, \tag{3}$$

where ρ_b and ρ_u denote burned gas and unburned gas densities, respectively, and u_b is the burned gas velocity at the end of the reaction zone. Therefore, one needs to know quantitatively the effect of radiation on both u_b and ρ_b/ρ_u.

The effect of radiation on flow velocity distribution is shown in Fig. 4 with R_{ch} = 10 cm and R_{ch} = 50 cm. The radial coordinate is normalized by each chamber radius as in Fig. 3. Fig. 4a shows that for adiabatic flames, $u_b = 0$ for R_{ch} = 50 cm while u_b is negative ($u_b < 0$) for R_{ch} = 10 cm. This difference is caused only by flow compression mentioned above. However, when the optically thin model is used, radiation loss results in negative burned gas velocity for both large and small chambers, and the effect is magnified for the case of smaller chamber size. This magnification of the negative burned gas velocity is an indication of the coupling between flow compression and radiation cooling. Therefore, accurate prediction of the negative burned gas effect requires the consideration of radiation.

The effect of radiation absorption on the negative u_b is predicted by using the FSNB-CK model for R_{ch} = 50 cm. Fig. 4b shows that development of gas velocity and the comparison with the result for R_{ch} = 10 cm. At 0.07 s, the FSNB-CK model predicts u_b = −3.7 cm/s, but the smaller chamber of 10 cm gives u_b = −14.5 cm/s at the same moment. Although not shown here, the optically thin model gives u_b = −16.6 cm/s at the same flame location for R_{ch} = 50 cm. As such, the optically thin model significantly over-predicts the negative burned gas velocity for an

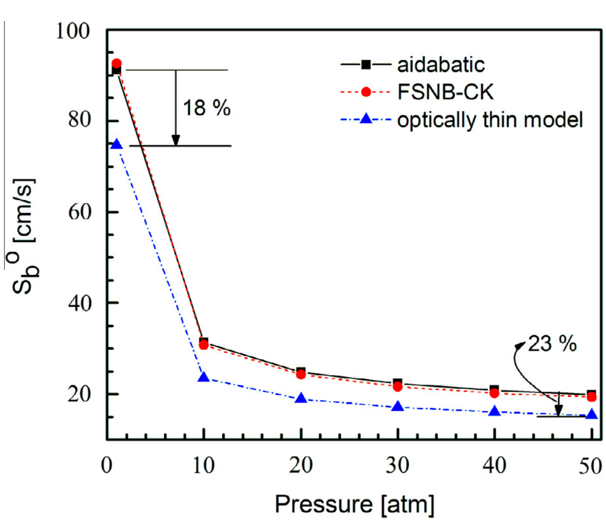

Fig. 2. Flame speeds as a function of pressure calculated with adiabatic, FSNB-CK, and optically thin models for $CH_4/O_2/He/CO_2$ flames in a spherical chamber of 10 cm radius.

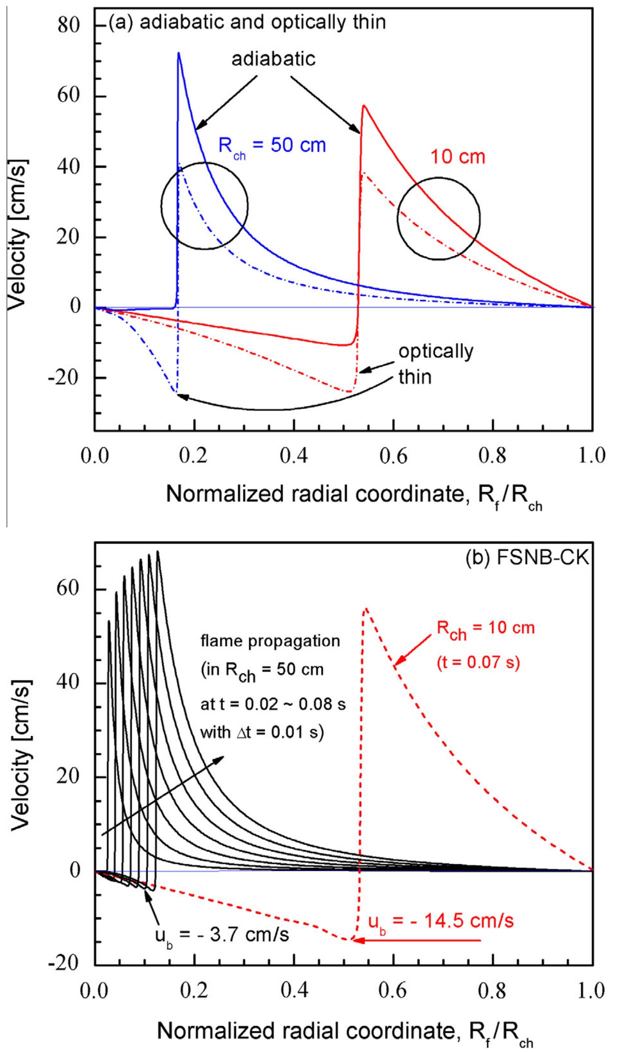

Fig. 4. Evolutionary velocity profiles along the radial coordinate calculated with (a) adiabatic and the optically thin models and (b) the FSNB-CK model for $CH_4/O_2/He/CO_2$ flames in a spherical chamber of 50 cm radius, which are compared with ones calculated in a smaller chamber of R_{ch} = 10 cm.

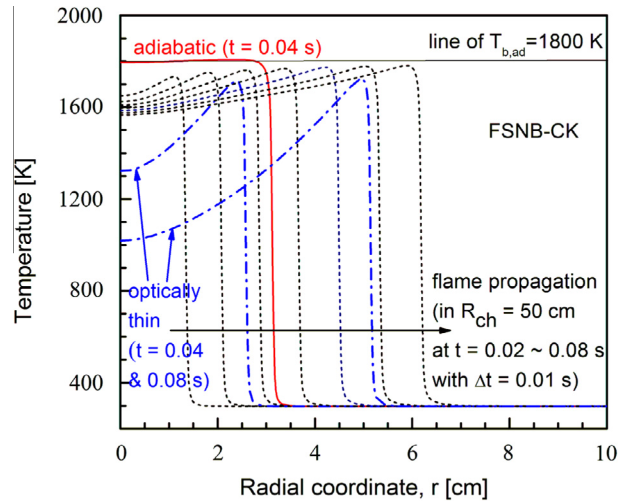

Fig. 5. Evolutionary temperature profiles along the radial coordinate calculated with adiabatic (solid line), optically thin (dash-dotted lines), and FSNB-CK (dashed lines) models for $CH_4/O_2/He/CO_2$ flames in a spherical chamber of 50 cm radius.

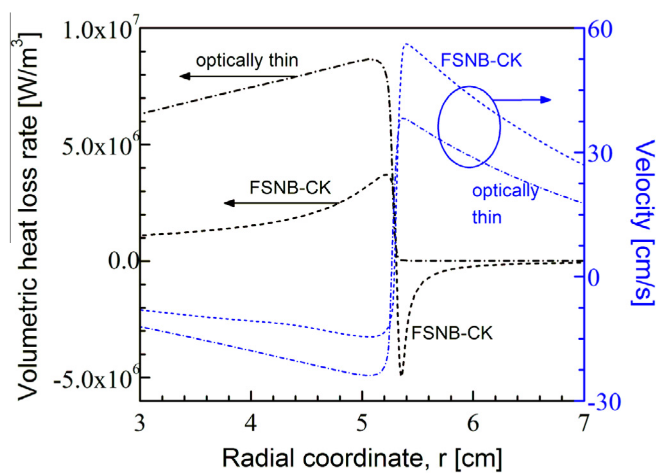

Fig. 6. Volumetric heat loss rate and velocity profiles along the radial coordinate calculated with the optically thin and the FSNB-CK models for $CH_4/O_2/He/CO_2$ flames in a spherical chamber of 10 cm radius.

optically thick mixture, especially with flow compression coupling in a small chamber.

Fig. 5 shows the evolution of temperature profiles calculated with the FSNB-CK model. The mixture has an adiabatic burned-gas temperature, $T_{b,ad}$, of 1800 K and density ratio, ρ_b/ρ_u, of 0.264 from thermodynamic equilibrium calculation. The FSNB-CK model predicts a decrease in temperature in the burned-gas region and reduced flame temperature at the end of the reaction zone. The optically thin model predicts more magnified decrease of temperature in the burned-gas region and the peak flame temperature. Therefore, the change in peak flame temperature will cause an increase of density ratio and modify the flame speed.

Fig. 6 shows distributions of volumetric radiative heat loss rate and velocity from two radiative models. In the burned-gas region, radiative heat loss of the optically thin model is above three times larger than that of the FSNB-CK model. Radiation (re-)absorption (negative radiative heat loss) is observed ahead of the flame front by the FSNB-CK model. These results indicate that the overestimation of heat loss and no absorption of the optically thin model render it not applicable to predict radiation in the optically thick mixture [14].

Fig. 4-6 suggest that flame speed should be corrected first by negative burned gas velocity (Eq. (3)). Flame speeds calculated with the FSNB-CK model at 1 atm are plotted as a function of stretch rate without and with the u_b-correction in Fig. 7. By u_b-correction, flame speeds are increased and the nonlinear dependence of flame speed on stretch rate shifts to lower stretch rate, which allows more accurate extrapolation of flame speed. The increase of $(S_b–u_b)^o$ is 4.8%. In addition to the u_b-correction, it is seen from Fig. 5 and Eq. (3) that the change of density ratio also affects the determination of flame speed. A recent work [30] reported that the burned-gas density is affected by curvature and non-unity Lewis number in flames with small radius and by confinement effect with large radius. With near-unity Lewis number, our attention here is paid only to density ratio (or flame temperature) change induced by radiation heat loss. Considering this additional correction, the unstretched flame speed should be expressed in the form,

$$S_L^o = \frac{\rho_{b,ad}}{\rho_u}\frac{T_{b,ad}}{T_b}(S_b - u_b)^o, \quad (4)$$

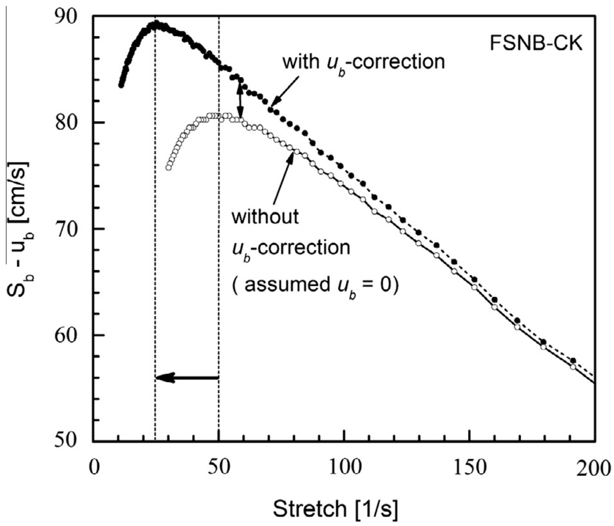

Fig. 7. Flame speeds calculated as a function of stretch without/with correction made by negative burned gas velocity, u_b, for $CH_4/O_2/He/CO_2$ flames in a spherical chamber of 10 cm radius.

where T_b denotes the peak burned-gas temperature from radiative calculation and $\rho_{b,ad}$ is the burned gas density of adiabatic flame. The former parameter, T_b, is determined to be the averaged value of the peak temperatures from temperature profiles over a time domain.

In summary, from Figs. 4–7 and Eq. (4), in order to obtain appropriately the flame speed from measurements/calculations of time-dependent flame trajectory of a spherical flame, two radiation-induced corrections are needed. One is the correction of negative velocity of the burned gas, u_b, and the other is consideration of change in density ratio. Table 1 shows the corrections at 1 atm, where the laminar flame speed, S_L^o, calculated from the FSNB-CK model, and its corrected values by negative u_b and increased density ratio as well as the flame speed calculated from the optically thin model. The S_L^o calculated by the FSNB-CK model without corrections is selected to be a baseline speed for this comparative study. The optically thin model underestimates the flame speed by 17.0%. The correction made by negative u_b increases the flame speed by 4.8% and the additional correction by the change of density ratio is 2.0%, making a total increase of 6.8%. The present result shows that the former correction is greater than the latter. This implies that the flame speed is decreased by thermal radiation by about 7% in an optically thick mixture. This correction may increase with the change of mixture composition. At elevated pressures up to 50 atm, the correction showed the similar level to one at 1 atm, but it decreased slightly with pressure, which indicates weak dependence of radiation-induced correction on pressure for the same mixture.

Table 1
Laminar flame speeds for $CH_4/O_2/He/CO_2$ flames with equivalence ratio of 0.6 at 1 atm predicted with and without radiation-induced velocity and density ratio corrections.

	FSNB-CK model without correction	FSNB-CK model – corrected by negative u_b	FSNB-CK model – corrected by negative u_b and density ratio	Optically thin modelwithout correction
Laminar flame speed, S_L^o [cm/s]	14.7	15.4	15.7	12.2
Correction to the FSNB-CK result	0	+4.8%	+6.8%	−17.0%

For this mixture, the measured, uncorrected flame speed was 13.1 cm/s at 1 atm [14], which is lower by 10.9% than the uncorrected laminar flame speed from the present numerical simulations. Accordingly, we can estimate that about 40% (=6.8/(6.8 + 10.9)) of the error is from radiative heat loss and the rest of it would be from inaccurate chemical kinetics and measurement error. The flame speed from the optically thin model is lower than the experimental data and is not valid for an optically thick mixture.

3.2. Flame propagation speeds of $H_2/O_2/He/H_2O/CO$ syngas mixture at elevated pressures

Typical oxygen blow coal derived syngas may contain large amount of water vapor as well as H_2, CO, N_2, and CO_2. A previous experiment [8] has reported the experimental data of flame speeds of syngas with water vapor and CO dilutions. However, the uncertainty due to radiation on flame speed is unknown. In a syngas, thermal radiation induced by H_2O and CO also affects flame propagation although the optical thickness may be smaller. In this study, a sample syngas, $H_2/O_2/He/H_2O/CO$ mixture [8] with optical thickness of about 0.3 at 1 atm, the initial temperature of 393 K, and the Lewis number for H_2 in the mixture of 1.08, is simulated and radiation effects on the flame speed are corrected by using Eq. (4).

Spherical flame propagation at pressures from 1 to 6 atm (experimental conditions [8]) was simulated using three radiation models. The uncorrected and corrected laminar flame speeds are shown as a function of pressure in Fig. 8 with predictions from the PREMIX code with adiabatic condition [31]. The corrections predicted by the FSNB-CK model vary from 2% to 4% at 1–6 atm, which is relatively smaller than ones predicted in the optically thick $CH_4/O_2/He/CO_2$ mixture. The correction decreases slightly with pressure and the corrected values are close to those predicted by the PREMIX code. The predicted errors by the optically thin model are 3%–10%, which is higher than that from the FSNB-CK model. By using Eq. (4), the experimental data were corrected by the same percentage as applied to the FSNB-CK model, resulting in the values marked as "EXP-corrected". At 1 atm, the corrected experimental value is closer to the laminar flame speed from the PREMIX code, but at higher pressures, the discrepancy is increased.

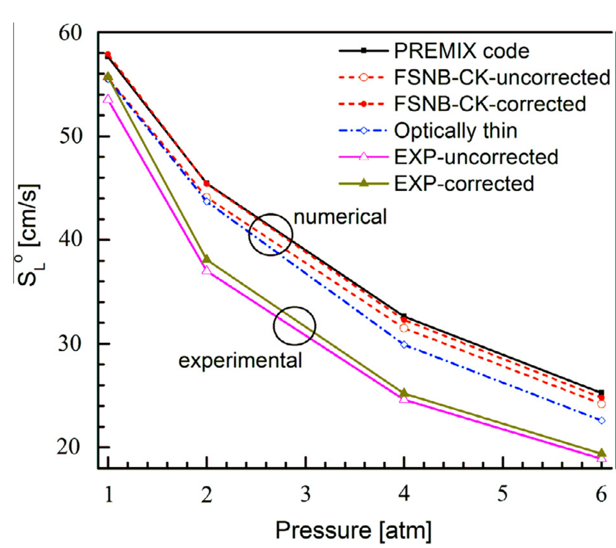

Fig. 8. Laminar flame speeds as a function of pressure calculated with the PREMIX code, two models of the FSNB-CK and the optically thin for $H_2/O_2/He/H_2O/CO$ flames in a spherical chamber of 10 cm radius, which are compared with experimental data [8] (data correction is made by both negative burned-gas velocity and increased density ratio).

The increased discrepancy between modeling and experiment with radiation correction might be due to the uncertainty of chemical kinetics at high pressure.

4. Conclusion

The spectral dependent radiation effects on the determination of flame speed from spherically propagating flames are numerically investigated by using the FSNB-CK model for an optically thick $CH_4/O_2/He/CO_2$ mixture and an optically thin $H_2/O_2/He/H_2O/CO$ mixture. The results show that radiation can cause a substantial uncertainty in flame speed measurements. Two radiation-induced effects on the flame speed determination were identified. The first effect is the radiation-induced negative burned gas velocity and the second one is the radiation-induced density ratio change. A correction method is proposed to take into account of these effects so that accurate flame speed can be obtained. Two different models, the optically thin model and the FSNB-CK model were used to assess the two radiation corrections to flame speed measurements.

The results show that the optically thin model over-predicts significantly the radiation correction for an optically thick mixture and is not valid for flame speed prediction, especially at elevated pressures. The FSNB-CK model predicts flame speeds close to the adiabatic value after correction. Due to the combined effect of radiation and flow compression, a smaller chamber causes a larger negative burned gas velocity and an earlier occurrence of nonlinear dependence of stretched flame speed on stretch rate at higher stretch rate, rendering the unstretched flame speed extrapolation more difficult. The results also show that density ratio change due to radiation reduces "measured" flame speed without proper correction. With the two-step radiation correction, the total increase in the flame speed is 6.8%, in which 4.8% from radiation induced negative burned gas velocity and 2% from the change of density ratio. Therefore, radiation correction is necessary for flame speed measurement in a spherical chamber for an optically thick mixture.

For an optically thin syngas mixture of $H_2/O_2/He/H_2O/CO$, radiation-induced flame speed correction is decreased to a few percentages. But, the optically thin model is not valid even for a mixture with optical thickness of 0.3. Therefore, in order to measure flame speed correctly for a radiative mixture, two radiation corrections need to be made and the spectral dependent radiation model needs to be used for appropriate radiation correction.

Conflict of interest

None declared

Acknowledgment

CHS was supported by the Power Generation & Electricity Delivery of the Korea Institute of Energy Technology Evaluation and Planning (KETEP) grant funded by the Korea government Ministry of Trade, Industry, and Energy (Project No. 2014101 010187C) and also supported by the National Research Foundation of Korea (NRF) grant funded by the Korean government (MEST) (NRF-2012S1A2A1A01031450). YJ and the computational code development were supported by the U.S. Department of Energy, Office of Basic Energy Sciences as part of an Energy Frontier Research Center on Combustion with Grant No. DE-SC0001198.

References

[1] J.E. Dec, Advanced compression-ignition engines understanding the in-cylinder processes, Proc. Combust. Inst. 32 (2009) 2727–2742.
[2] T. Tsurushima, A new skeletal PRF kinetic model for HCCI combustion, Proc. Combust. Inst. 32 (2009) 2835–2841.
[3] R.D. Reitz, Directions in internal combustion research, Combust. Flame 160 (2013) 1–8.
[4] M.P. Burke, M. Chaos, Y. Ju, F.L. Dryer, S.J. Klippenstein, Comprehensive H_2/O_2 kinetic model for high-pressure combustion, Int. J. Chem. Kinet. 44 (2012) 444–474.
[5] A. Kéromnès, W.K. Metcalfe, K.A. Heufer, N. Donohoe, A.K. Das, C.-J. Sung, J. Herzler, C. Naumann, P. Griebel, O. Mathieu, M.C. Krejci, E. Petersen, W.J. Pitz, H.J. Curran, An experimental and detailed chemical kinetic modeling study of hydrogen and syngas mixture oxidation at elevated pressures, Combust. Flame 160 (2013) 995–1011.
[6] M.P. Burke, M. Chaos, F.L. Dryer, Y. Ju, Negative pressure dependence of mass burning rates of $H_2/CO/O_2$/diluent flames at low flame temperatures, Combust. Flame 157 (2010) 618–631.
[7] X. Qin, Y. Ju, Measurements of burning velocities of dimethyl ether and air premixed flames at elevated pressures, Proc. Combust. Inst. 30 (2005) 233–240.
[8] J. Santner, F.L. Dryer, Y. Ju, The effects of water dilution on hydrogen, syngas, and ethylene flames at elevated pressure, Proc. Combust. Inst. 34 (2013) 719–726.
[9] S.D. Tse, D.L. Zhu, C.K. Law, Morphology and burning rates of expanding spherical flames in H_2/O_2/inert mixtures up to 60 atmospheres, Proc. Combust. Inst. 28 (2000) 1793–1800.
[10] Z. Chen, M.P. Burke, Y. Ju, Effects of compression and stretch on the determination of laminar flame speeds using propagating spherical flames, Combust. Theory Model. 13 (2009) 343–364.
[11] Z. Chen, On the extraction of laminar flame speed and Markstein length from outwardly propagating spherical flames, Combust. Flame 158 (2012) 291–300.
[12] A.P. Kelley, J.K. Bechtold, C.K. Law, Premixed flame propagation in a confining vessel with weak pressure rise, J. Fluid Mech. 691 (2012) 26–51.
[13] Y. Ju, G. Masuya, P.D. Ronney, Effects of radiative emission and absorption on the propagation and extinction of premixed gas flames, Proc. Combust. Inst. 27 (1998) 2619–2626.
[14] Z. Chen, X. Qin, B. Xu, Y. Ju, F. Liu, Studies of radiation absorption on flame speed and flammability limit of CO_2 diluted methane flames at elevated pressures, Proc. Combust. Inst. 31 (2007) 2693–2700.
[15] H. Yu, W. Han, J. Santner, X. Gou, C.H. Sohn, Y. Ju, Z. Chen, Radiation-induced uncertainty in laminar speed measured from propagating spherical flames, Combust. Flame 161 (2014) 2815–2824.
[16] Z. Chen, Effects of radiation and compression on propagating spherical flames of methane/air mixtures near the lean flammability limit, Combust. Flame 157 (2010) 2267–2276.
[17] J. Santner, F.M. Haas, Y. Ju, F.L. Dryer, Uncertainties in interpretation of high pressure spherical flame propagation rates due to thermal radiation, Combust. Flame 161 (2014) 147–153.
[18] Z. Chen, Studies on the initiation, propagation, and extinction of premixed flames (Ph.D. thesis), Princeton University, NJ, USA, 2008.
[19] Z. Chen, M.P. Burke, Y. Ju, Effects of Lewis number and ignition energy on the determination of laminar flame speed using propagating spherical flames, Proc. Combust. Inst. 32 (2009) 1253–1260.
[20] Z. Chen, M.P. Burke, Y. Ju, On the critical flame radius and minimum ignition energy for spherical flame initiation, Proc. Combust. Inst. 33 (2011) 1219–1226.
[21] Y. Ju, H. Guo, F. Liu, K. Maruta, Effects of the Lewis number and radiative heat loss on the bifurcation and extinction of CH_4/O_2-N_2-He flames, J. Fluid Mech. 379 (1999) 165–190.
[22] C.L. Tien, Thermal radiation properties of gases, Adv. Heat Transfer 5 (1968) 253–324.
[23] A.A. Lacis, V.A. Oinas, A description of the correlated k distribution method for modeling nongray gaseous absorption, thermal emission, and multiple scattering in vertically inhomogeneous atmospheres, J. Geophys. Res. 96 (1991) 9027–9063.
[24] A. Soufiani, J. Taine, High temperature gas radiative property parameters of statistical narrow-band model for H_2O, CO_2 and CO, and correlated-K model for H_2O and CO_2, Int. J. Heat Mass Trans. 40 (1997) 987–991.
[25] J.W. Son, S.H. Kim, C.H. Sohn, On burnout performance of a rocket-engine-based incinerator devised for high burning rate of solid particles, Fuel 117 (2014) 478–487.
[26] J.W. Son, C.H. Sohn, Evaluation of burnout performance of biomass wastes in a rocket-engine-based incinerator, Fuel 143 (2015) 308–317.
[27] Available at http://www.me.berkeley.edu/gri_mech/.
[28] J. Li, A. Kazakov, Z. Zhao, M. Chaos, F.L. Dryer, J.J. Scire, A comprehensive kinetic mechanism for CO, CH_2O, and CH_3OH combustion, Int. J. Chem. Kinet. 39 (2007) 109–136.
[29] R.J. Kee, F.M. Rupley, J.A. Miller, CHEMKIN-II: A General-Purpose, Problem-independent, Transportable, Fortran Chemical Kinetics Code Package, Report No. SAND89-8009B, Sandia National Laboratories, Livermore, CA, 1989.
[30] A. Bonhomme, L. Selle, T. Poinsot, Curvature and confinement effects for flame speed measurements in laminar spherical and cylindrical flames, Combust. Flame 160 (2013) 1208–1214.
[31] R.J. Kee, J.F. Grcar, M.D. Smooke, J.A. Miller, Fortran Program for Modeling Steady Laminar one dimensional Premixed Flames, Report No. SAND85-8240, Sandia National Laboratories, Livermore, CA, 1985.